COMBINED EFFECTS OF VARIABLE VISCOSITY AND THERMOPHORETIC TRANSPORTATION ON MIXED CONVECTION FLOW AROUND THE SURFACE OF A SPHERE

by

Amir ABBAS and Muhmmad ASHRAF*

Department of Mathematics, Faculty of Science, University of Sargodha, Sargodha, Pakistan

Original scientific paper
https://doi.org/10.2298/TSCI190518137A

The physical behavior of the combined effect of temperature dependent viscosity and thermophoretic motion on mixed convection flow around the surface of a sphere is investigated. The set of non-linear coupled PDE is formulated and then non-dimensionalized by using an appropriate set of dimensionless variables. The dimensionless model is then transformed to convenient form for integration by employing a suitable set of primitive variables formulation and then discretized by using an efficient implicate finite difference scheme for numerical simulation. The effect of controlling parameters on velocity profile, temperature profile, and mass concentration as well as skin friction, rate of heat transfer, and mass transfer rate are analyzed. The obtained numerical results for different values of controlling parameters indicate that, velocity profile gains its largest magnitude at position $X = 1.5$ radian and slows down at postion $X = \pi$ radian. It is also predicted that the temperature distribution and mass concentration are diluted at position $X = 1.5$ radian due to rapid motion of fluid. The numerical results are highlighted in graphical as well as in tabular form.

Key words: *thermophoretic transportation, temperature dependent viscosity, mixed convection, sphere, implicate finite difference method*

Introduction

The thermophoretic transportation is the phenomenon in which submicron particles move away or come towards the surface due to temperature gradient. The force through which these particles gain momentum is known as thermophoretic force. Several applications of the thermophoretic motion are seen in industry and engineering like cleaning of air, microelectronic manufacturing processes, scale formation on the surfaces of heat exchangers and nuclear reactors safety. Sphere shaped metals and alloys are major requirements of industry. The study of mixed convection flow and thermophoretic transportation due to their wide range of applications received the attention of many scientist and researchers. Potter and Riley [1] studied the phenomenon of eruption of fluid from boundary-layer into the plume above the sphere. Epstein *et al.* [2] analyzed the effect of thermophoretic force on convective heat transfer due to deposition of thermophoretic particles on a vertical cold surface numerically. Attia [3] discussed the phenomenon of unsteady flow of dusty fluid through an electrically conducting fluid along an infinite flat plate in the presence of magnetic field with the inclusion of temperature dependent viscosity and thermal conductivity. She con-

* Corresponding author, e-mail: muhammad.ashraf@uos.edu.pk

cluded that as the values of thermal conductivity parameter are increased by taking the positive values of temperature dependent viscosity parameter, the velocities of the fluid and dust particles increased and vice versa. Chin *et al.* [4] reported the study of steady mixed convection flow over a vertical porous plate embedded in porous media influenced by variable viscosity. They came to the conclusion that boundary-layer separation slows down when parameter defining the effect of variable viscosity $\theta_e > 0$ than that $\theta_e < 0$. El-Hakiem and Rashad [5] investigated numerically the combined effects of radiation and non-linear Forchheimer terms on free convection flow along a cylinder embedded in fluid saturated porous medium. Enzo [6] focused on the phenomenon of laminar mixed convection flow in a vertical annular duct comprising on a constant temperature under the effect of variable viscosity analytically. He came to the conclusion that the buoyancy forces and temperature dependent viscosity have significant effects on fanning friction. An analysis on the continuous problem of the uncoupled steady momentum and energy equations by taking the effect of the temperature dependent viscosity into account has been performed by Perez *et al.* [7]. Perez *et al.* [8] examined the discrete problem of steady momentum and energy equations and performed some numerical simulations for both steady and unsteady cases. Aziz and Rania [9] discussed the effect of temperature dependent viscosity on heat- and fluid-flow mechanism over a permeable stretched surface. They concluded that the increasing value of viscosity variation parameter leads to the reduction in velocity distribution, and suction of surface leads to increase in Nusselt number while injection showed opposite effect with the increasing value of Prandtl number. Chamkha *et al.* [10] proposed the study of heat and mass transfer around the vertical cylinder by considering the effect of radiation and chemical reaction with temperature dependent viscosity. They predicted that local Nusselt number decreased as conduction radiation parameter and Lewis number are increased, while the local Nusselt number decreased and local Sheward number increased for higher values of chemical reaction parameter. On the other hand, they found that the fluid motion accelerated by increasing the values of variable viscosity. Rashad *et al.* [11] discussed the phenomenon of heat- and fluid-flow around a sphere in a saturated porous medium. They encountered the influence of chemical reaction and solved the governing model by using implicit finite difference method.

Chinyoka and Makinde [12] focused on heat transfer and fluid-flow of electrically conducting third-grade fluid under the influence of variable viscosity and transverse magnetic field. They illustrated that fluid velocity and temperature profiles increased transiently as viscous heating, fluid viscosity, and reaction strength improved. Hayat *et al.* [13] gave the idea of the problem of mixed convection peristaltic flow of an electrically conducting fluid on inclined channel under the influence of temperature dependent viscosity and thermal conductivity. They computed, pressure gradient, velocity, rate of heat transfer, and streamlines by using some numerical technique. Crosby and Lister [14] extended the idea of Olsun to study the steady axisymmetric thermal plumes erupting form a very viscous fluid considering the effect of temperature dependent viscosity of the form $\mu \propto \exp(-\gamma T)$. They concluded that temperature decreased exponentially and decay was faster than that existing in previous literature. Dhiman and Sharma [15] analyzed the effect of temperature dependent viscosity on thermal convection in nanofluids. They obtained the expression of Raleigh number for the cases of linear and exponential viscosity parameter by using weighted residual method. They computed and presented the numerical results in tabular form for the different values of wave number, viscosity variation parameter and fixed values of Lewis number and concentration Rayleigh number. The effect of wall heating on thermal boundary over isothermally heated wall have been discussed by Lee *et al.* [16] by using direct numer-

ical simulation technique. They predicted that mean wall normal velocity and normal scalar flux leads to increase the heat transfer coefficient. Umavathi and Ojjela [17] investigated that the temperature contours remains linear for all values of viscosity variation parameter. The effect of variable viscosity and thermal conductivity along magnetized surface have been explored by Ashraf *et al* [18]. They illustrated that velocity boundary-layer is increased and there was no change noted in thermal and magnetic boundary-layers for higher values of viscosity variation parameter. Thoray and Michaut [19] investigated numerically the behavior of cooling elastic gravity currents for influx conditions incorporating the effect of temperature dependent viscosity. Makinde *et al.* [20] carried out the analysis on MHD convective heat and mass transfer taking the effect of thermophoresis radiation and temperature dependent viscosity and predicted that skin friction decreases and Nusselt number increases for increasing values of temperature dependent viscosity. Malikarjuna *et al*. [21] studied theoretically the combined effect of thermophoresis, thermal radiation and transpiration on convective flow through rotating cone. A comprehensive analysis on periodic mixed convection flow along the surface of a sphere under the influence of viscous dissipation has been carried out by Ashraf *el al.* [22], and governing equations have been solved by using implicit finite difference scheme. Ashraf and Fatima [23] also presented the numerical simulation based on finite difference method to study the effect of shear stress and rate of heat transfer around different positions of sphere associated with the fluid dissipation. They paid a special attention on the behavior of transient shear stress and heat transfer rate under the influence of dimensionless parameters appeared in the flow model. Later, Ashraf *el al.* [24], extended the work of Potter [1] for nanofluid heat transfer around different stations of sphere and into plume above the sphere.

To our knowledge, there exists no literature on the analysis of the combined effects of variable viscosity and thermophoretic transportation on mixed convection flow around the surface of a sphere. In this paper, this combined effect on thermal transport phenomena for higher values of Prandtl number along with other parametres involved in flow model is explored. In particular, we contribute, how the physical behavior of velocity profile, temperature distribution, mass concentration, skin friction, heat transfer, and mass flux is behaved around the surface of sphere at different positions.

Mathematical formulation

A sphere of radius, a, is held at temperature, T_w, mass concentarion, C_w, and immersed in a viscous incompressible fluid with ambient temperature, T_∞, ambient mass concentration C_∞ and free stream velocity U_∞ by assuming $T_w > T_\infty$ and $C_w > C_\infty$. To analyses the boundary-layer behavior of heat- and fluid-flow with the inclusion of thermophoretic transportation around the surface of sphere no slip condition that is $u = 0$ and $v = 0$ is applied. Co-ordinate system and flow configuration is given in fig. 1. In keeping view the characteristics of fluid and fluid-flow domain the mathematical model represents the fluid-flow behavior in terms of dimensionless non-linear PDE are given:

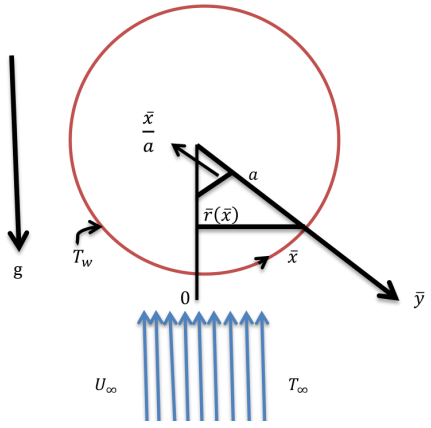

Figure 1. Co-ordinate system and flow confuguration

$$\frac{\partial(\sin x\, u)}{\partial x}+\frac{\partial(\sin x\, v)}{\partial y}=0 \tag{1}$$

$$u\frac{\partial u}{\partial x}+v\frac{\partial u}{\partial y}=\frac{1}{(1+\epsilon\theta)}\frac{\partial^2 u}{\partial y^2}-\frac{\varepsilon}{(1+\varepsilon\theta)^2}\frac{\partial u}{\partial y}\frac{\partial\theta}{\partial y}+\lambda_t\theta\sin x+\lambda_c\phi\sin x \tag{2}$$

$$u\frac{\partial\theta}{\partial x}+v\frac{\partial\theta}{\partial y}=\frac{1}{\mathrm{Pr}}\frac{\partial^2\theta}{\partial y^2} \tag{3}$$

$$u\frac{\partial\phi}{\partial x}+v\frac{\partial\phi}{\partial y}=\frac{1}{\mathrm{Sc}}\frac{\partial^2\phi}{\partial y^2}-\frac{\partial(v_t\phi)}{\partial y} \tag{4}$$

where the dimensionless variables are defined in below:

$$x=\frac{\overline{x}}{a},\quad y=\frac{\overline{y}\,\mathrm{Re}^{1/2}}{a},\quad \theta=\frac{T-T_\infty}{T_\infty-T_\mathrm{w}},\quad \phi=\frac{C-C_\infty}{C_\infty-C_\mathrm{w}}$$

$$u=\frac{\overline{u}}{U_\infty},\quad v=\frac{\overline{v}\,\mathrm{Re}^{1/2}}{U_\infty},\quad v_t=\frac{\overline{v}_t\,\mathrm{Re}^{1/2}}{U_\infty},\quad \mu=\frac{\mu_\infty}{1+\gamma^*(T-T_\infty)} \tag{5}$$

Here, $\epsilon=\gamma^*\Delta T$ is viscosity variation parameter and γ^* is constant. The dimensionless parameters $\lambda_t=\mathrm{Gr}_t/\mathrm{Re}^2$, $\lambda_c=\mathrm{Gr}_c/\mathrm{Re}^2$, $\mathrm{Gr}_t=\mathrm{g}\beta_t(T-T_\infty)a^3/\nu^2$, $\mathrm{Gr}_c=\mathrm{g}\beta_c(C-C_\infty)a^3/\nu^2$, $\mathrm{Re}=U_\infty a/\nu$, $\mathrm{Pr}=\nu/\alpha$, and $\mathrm{Sc}=\nu/D_m$ are mixed convection parameter, modified mixed convection parameter, Grashof number, modified Grashof number, Reynolds number, Prandtl number, and Schmidt number, respectively. In boundary-layer flow, the temperature along the y-co-ordinate is much larger than that in the x-co-ordinate, and that is why, the thermophoretic velocity in y-direction is considered. As a consequence, the thermophoretic velocity, which is appearing in eq. (4) can be expressed in the form:

$$v_t=-\frac{k}{\theta+Nt}\frac{\partial\theta}{\partial y}$$

here θ is dimensionless temperature, k – the thermophoretic coefficient, and $Nt=\Delta T/T_\infty$ – the thermophoresis parameter. Corresponding boundary conditions satisfied by the previous system of PDE are given:

$$\begin{aligned} &u=0,\quad v=0,\quad \theta=1,\quad \phi=1,\quad \text{at}\quad y=0\\ &u\to 1,\quad \theta\to 0,\quad \phi\to 0,\quad \text{as}\quad y\to\infty \end{aligned} \tag{6}$$

Solution methodology

To transform the system of eqs. (1)-(5) along with their boundary conditions (6) into convenient form for integration, we use the idea of primitive variable formulation. The group of primitive variable formulation of the dependent and independent variables as studied in [18-20] are given:

$$\begin{aligned} &u(x,y)=U(X,Y),\quad v(x,y)=x^{-1/2}V(X,Y)\\ &Y=x^{-1/2}y,\quad X=x,\quad v_t(x,y)=x^{-1/2}V_t(X,Y)\\ &\theta(x,y)=X^{-1}\theta(X,Y),\quad \phi(x,y)=X^{-1}\phi(X,Y) \end{aligned} \tag{7}$$

By using eq. (7) into eqs. (1)-(5) along with corresponding boundary conditions (6), we obtain the following transformed system of coupled PDE:

$$XU\cos X+\left(X\frac{\partial U}{\partial X}-\frac{Y}{2}\frac{\partial U}{\partial Y}+\frac{\partial V}{\partial Y}\right)\sin X=0 \tag{8}$$

$$XU\frac{\partial U}{\partial X}+\left(V-\frac{YU}{2}\right)\frac{\partial U}{\partial Y}=\frac{X}{\left(X+\varepsilon\theta\right)}\frac{\partial^2 U}{\partial Y^2}-\frac{\varepsilon X}{\left(X+\varepsilon\theta\right)^2}\frac{\partial U}{\partial Y}\frac{\partial\theta}{\partial Y}+\lambda_t\sin X\,\theta+\lambda_c\sin X\,\phi \tag{9}$$

$$XU\frac{\partial\theta}{\partial X}+\left(V-\frac{YU}{2}\right)\frac{\partial\theta}{\partial Y}-\theta U=\frac{1}{\mathrm{Pr}}\frac{\partial^2\theta}{\partial Y^2} \tag{10}$$

$$XU\frac{\partial\phi}{\partial X}+\left(V-\frac{YU}{2}\right)\frac{\partial\phi}{\partial Y}-\phi U=\frac{1}{\mathrm{Sc}}\frac{\partial^2\phi}{\partial Y^2}-\frac{\partial(V_t\phi)}{\partial Y} \tag{11}$$

where

$$V_t=-\frac{k}{\theta+XNt}\frac{\partial\theta}{\partial Y}$$

Corresponding transformed boundary conditions are:

$$\begin{gathered}U=0,\quad V=0,\quad \theta=1,\quad \phi=1,\quad \text{at}\quad Y=0\\ U\to 1,\quad \theta\to 0,\quad \phi\to 0,\quad \text{as}\quad Y\to\infty\end{gathered} \tag{12}$$

Computational technique

The transformed system of eqs. (8)-(12) are discretized by using the finite difference scheme, central difference along y-axis and back difference along x-axis. The discretization-process in detailed is given:

$$\frac{\partial U}{\partial X}=\frac{U_{(i,j)}-U_{(i,j-1)}}{\Delta X} \tag{13}$$

$$\frac{\partial U}{\partial Y}=\frac{U_{(i+1,j)}-U_{(i-1,j)}}{2\Delta Y} \tag{14}$$

$$\frac{\partial^2 U}{\partial Y^2}=\frac{U_{(i+1,j)}-2U_{(i,j)}+U_{(i-1,j)}}{\Delta Y^2} \tag{15}$$

Putting eqs. (13)-(15) in eqs. (8)-(12), we obtain the following system of algebraic equations:

– form of continuity equation:

$$\begin{gathered}V_{(i+1,j)}=V_{(i-1,j)}-2\frac{\Delta Y}{\Delta X}X_i\left[U_{(i,j)}-U_{(i,j-1)}\right]+\frac{Y_j}{2}\left[U_{(i+1,j)}-U_{(i-1,j)}\right]-\\ -2\Delta Y X_i\frac{\cos X_i}{\sin X_i}U_{(i,j)}\end{gathered} \tag{16}$$

– form of momentum equation:

$$A_1U_{(i-1,j)}+B_1U_{(i,j)}+C_1U_{(i+1,j)}=D_1 \tag{17}$$

where

$$A_1 = \frac{X_i}{(X_i + \varepsilon\theta_{i,j})} + \left\{ \frac{\Delta Y}{2}\left[V_{(i,j)} - \frac{Y_j}{2} U_{(i,j)} \right] + \frac{\varepsilon X_i}{4\left[X_i + \varepsilon\theta_{(i,j)} \right]^2} \left[\theta_{(i+1,j)} - \theta_{(i-1,j)} \right] \right\}$$

$$B_1 = -\frac{2X_i}{(X_i + \varepsilon\theta_{i,j})} - \frac{\Delta Y^2}{\Delta X} X_i U_{(i,j)}$$

$$C_1 = \frac{X_i}{(X_i + \varepsilon\theta_{i,j})} - \left\{ \frac{\Delta Y}{2}\left[V_{(i,j)} - \frac{Y_j}{2} U_{(i,j)} \right] + \frac{\varepsilon X_i}{4\left[X_i + \varepsilon\theta_{(i,j)} \right]^2} \left[\theta_{(i+1,j)} - \theta_{(i-1,j)} \right] \right\}$$

$$D_1 = -\Delta Y^2 \sin X_i \left[\lambda_t \theta_{(i,j)} + \lambda_c \phi_{(i,j)} \right] - \frac{\Delta Y^2}{\Delta X} X_i U_{(i,j)} U_{(i,j-1)}$$

– form of energy equation:

$$A_2\theta_{(i-1,j)} + B_2\theta_{(i,j)} + C_2\theta_{(i+1,j)} = D_2 \tag{18}$$

where

$$A_2 = \frac{1}{\mathrm{Pr}} + \frac{\Delta Y}{2}\left[V_{(i,j)} - \frac{Y_j}{2} U_{(i,j)} \right]$$

$$B_2 = -\frac{2}{\mathrm{Pr}} + \Delta Y^2 U_{(i,j)} \left(1 - \frac{X_i}{\Delta X} \right)$$

$$C_2 = \frac{1}{\mathrm{Pr}} - \frac{\Delta Y}{2}\left[V_{(i,j)} - \frac{Y_j}{2} U_{(i,j)} \right]$$

$$D_2 = -\frac{\Delta Y^2}{\Delta X} X_i U_{(i,j)} \theta_{(i,j-1)}$$

– form of mass transportation equation:

$$A_3\phi_{(i-1,j)} + B_3\phi_{(i,j)} + C_3\phi_{(i+1,j)} = D_3 \tag{19}$$

$$A_3 = \frac{1}{\mathrm{Sc}} + \frac{\Delta Y}{2}\left[V_{t(i,j)} + V_{(i,j)} - \frac{Y_j}{2} U_{(i,j)} \right]$$

$$B_3 = -\frac{2}{\mathrm{Sc}} + \Delta Y^2 U_{(i,j)} \left(1 - \frac{X_i}{\Delta X} \right)$$

$$C_3 = \frac{1}{\mathrm{Sc}} - \frac{\Delta Y}{2}\left[V_{t(i,j)} + V_{(i,j)} - \frac{Y_j}{2} U_{(i,j)} \right]$$

$$D_3 = -\frac{\Delta Y^2}{\Delta X} X_i U_{(i,j)} \phi_{(i,j-1)}$$

The discretized form of thermophoretic velocity is:

$$V_{t(i,j)} = -\frac{k}{\theta_{(i,j)} + X_i N_t} \frac{\theta_{(i+1,j)} - \theta_{(i-1,j)}}{2\Delta Y}$$

Corresponding boundary conditions are:

$$\begin{gathered} U_{(i,j)} = 0, \quad V_{(i,j)} = 0, \quad \theta_{(i,j)} = 1, \quad \phi_{(i,j)} = 1, \quad \text{as} \quad Y_j = 0 \\ U_{(i,j)} \to 1, \quad \theta_{(i,j)} \to 0, \quad \phi_{(i,j)} \to 0, \quad \text{as} \quad Y_j \to \infty \end{gathered} \tag{20}$$

The previous system of algebraic equations is solved by using Gaussian elimination technique. Here the variables U, V, θ and ϕ are unknown variables. We find the values of these variables at each mesh point by solving coefficient matrix. The values of these variables represent velocity profile, temperature distribution and mass concentration against normal distance Y, further the derivatives of these variables represent skin friction, heat transfer, and mass flux around the surface of a sphere. The matrix form of the system of algebraic equations is simulated by using computer software Lahy Fortran-95 and the obtained data is plotted with the help graphical software Tecplot-360. Further, the accuracy of the obtained numerical results can be observed from figs. 2-8. In these figures the obtained numericalcal results are satisfied by the given boundary conditions. Moreover, a remarkable asymptotic behavior in each figure has calculated which indicates that we have captured skin friction, heat transfer and mass flux accurately.

Results and discussion

In the present study, computational analysis for velocity profile, temperature distribution,mass concentration, skin friction as well as rate of heat transfer, mass flux has been carried out under the combined effects of temperature dependent viscosity and thermophoretic transportation. The behavior of the main physical quantities under the influence of governing parameters is displayed graphically as well as in tabular form. The effect of viscosity variation parameter, mixed convection parameter, modified mixed convection parameter, Prandtl number, Schmidt number, thermophoretic coefficient, and thermophoresis parameter are taken into account to glean at the behavior of aforementioned physical quantities. The detailed interpretation of the governing quantities is presented in tables and the graphs plotted as below.

The effect of various values of viscosity variation parameter ε upon the velocity profile, temperature profile, and mass concentration as well as skin friction, rate of heat transfer, and mass flux, at different circumferential positions of a sphere are displayed in figs. 2(a)-2(c).

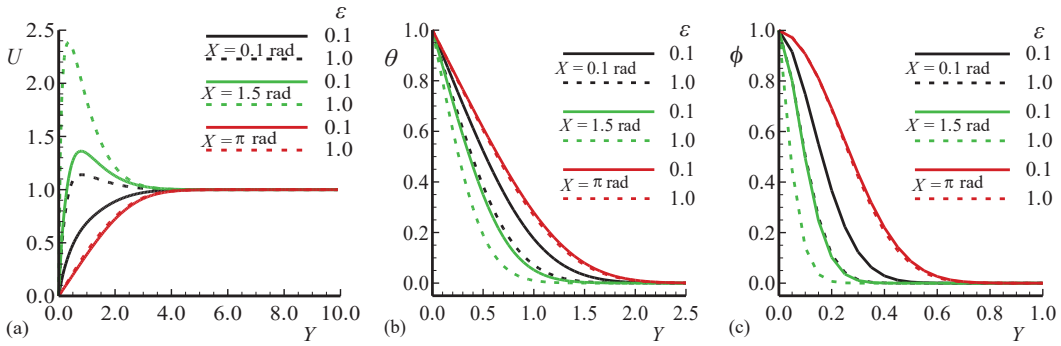

Figure 2. Graphical results of; (a) velocity profile (b) temperature profile, and (c) mass concentration against Y for different values of ε = 0.1, 1.0, when other parameters λ_t = 10.0, λ_c = 10.0, Pr = 7.0, Sc = 10.0, k = 1.0, and Nt = 10.0 are constant (*for color image see journal web site*)

It is noted from the figs. 2(a)-2(c), that velocity profile increases owing to increase in viscosity variation parameter but the opposite behavior is seen in temperature distribution and mass concentration. The velocity of the fluid is maximum at position $X = 1.5$ radian, but temperature distribution and mass concentration attain maximum momentum at position $X = \pi$ radian, respectively. It is of interest to note that enhancement in the viscosity variation parameter increase the temperature difference which accelerates the fluid motion at the center while the mass concentration and temperature are prominent at lower region.

The results in figs. 3(a)-3(c) illustrate the effect of thermophoresis parameter, *Nt*, on velocity profile, temperature distribution and mass concentration, respectively. It is revealed from figs. 3(a)-3(c) that the fluid velocity is increased significantly for higher values of thermophoresis parameter *Nt* by keeping the other parameters constant. On the other hand, opposite behavior can be seen in temperature profile and mass concentration. It is important to note that no significant change in temperature is found at position $X = \pi$ radian, but mass concentration substantially increases at the same position. This is due to the fact that the increase in thermophoresis parameter decreases the ambient temperature and surface loses its more temperature to ambient region around the sphere.

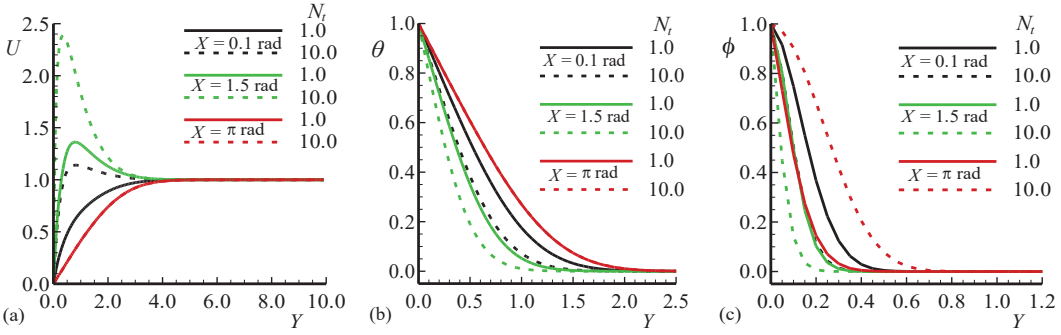

Figure 3. Graphical results of; (a) velocity profile (b) temperature profile, and (c) mass concentration against *Y* for different values of *Nt* = 1.0, 10.0, when other parameters $\varepsilon = 0.8$, $\lambda_t = 10.0$, $\lambda_c = 1.0$, Pr = 7.0, Sc = 10.0, and *k* = 1.0 are kept constant (*for color image see journal web site*)

Figures 4(a)-4(c) compute the effect of Prandtl number over velocity profile, temperature distribution and mass concentration around a sphere at different three positions. From these figures it is noted that velocity of the fluid is increased at position $X = 1.5$ and gains its maximum value for Pr = 0.71, while the temperature and mass concentration are reduced at the same position. It is also fair to note that temperature at position $X = 1.5$ radian is maximum for Pr = 0.71. It is also observed that temperature distribution is decreased and mass concentration is increased for increasing values of Prandtl number at position $X = \pi$ radian. It is obvious because fluids with lower Prandtl number are good heat conductor. The increase in Schmidt number tends to increase the velocity profile at position $X = 1.5$ radian and reverse phenomena at same position for the case of temperature distribution and mass concentration is noted in figs. 5(a)-5(c). It is also noted that temperature distribution is reduced and mass concentration is enhanced for increasing values of Schmidt number. Further, it is observed that no change is recorded in temperature distribution at position $X = \pi$ radian, but on the other side, the mass concentarion very prominently increased for increasing values of Schmidt number at the same postion $X = \pi$ radian of the sphere. This is due to the reason that the higher range of Schmidt number leads to reduce the viscosity of the fluid and produced maximum inertial force which supports the above said mechanism.

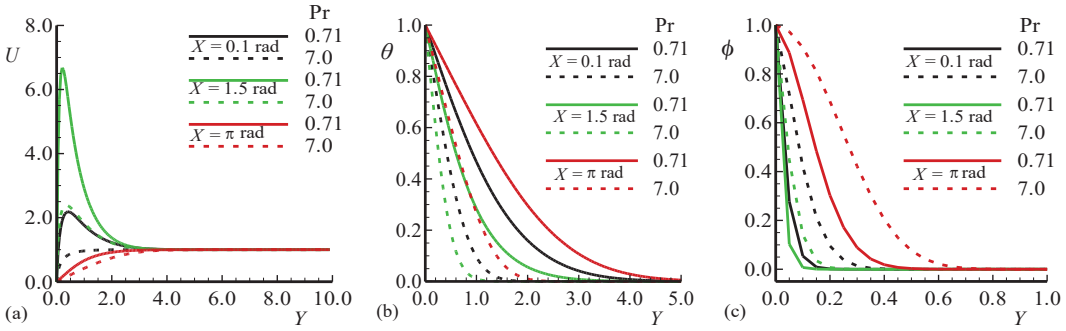

Figure 4. Graphical results of; (a) velocity profile (b) temperature profile, and (c) mass concentration against Y for different values of Pr = 0.71, 7.0, when other parameters $Nt = 10.0$, $\varepsilon = 1.0$, $\lambda_t = 10.0$, $\lambda_c = 1.0$, Sc = 10.0, and $k = 1.0$ are kept constant (*for color image see journal web site*)

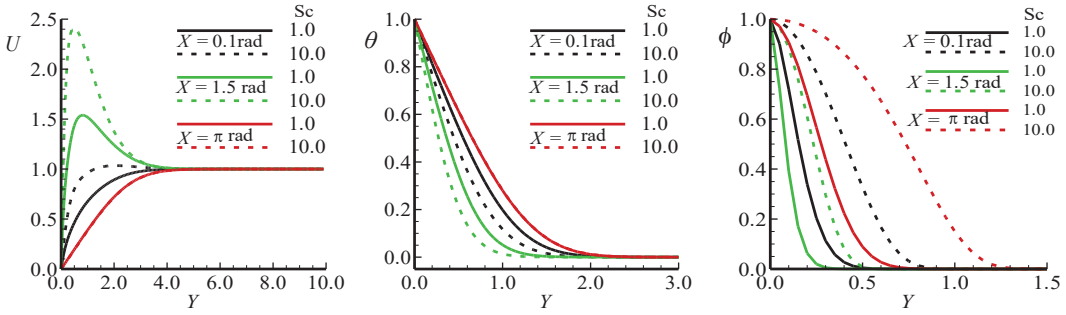

Figure 5. Graphical results of; (a) velocity profile (b) temperature profile, and (c) mass concentration against Y for different values of Sc = 1.0, 10.0, when other parameters Pr = 7.0, $Nt = 10.0$, $\varepsilon = 2.0$, $\lambda_t = 10.0$, $\lambda_c = 10.0$ and $k = 1.0$ are constant (*for color image see journal web site*)

Figures 6(a)-6(c) show the corresponding change in the profiles of variables U, θ, and ϕ for the increasing values of mixed convection parameter λ_t. In these figures maximum fluid motion is predicted at postion $X = 1.5$ and having a meaningful peak for $\lambda_t = 5.0$, while the temperature distribution and mass concentarion is higher at position $X = \pi$ radian with no difference due to the increasing values of λ_t. Figure 6(a) is a reasonable answer to the question

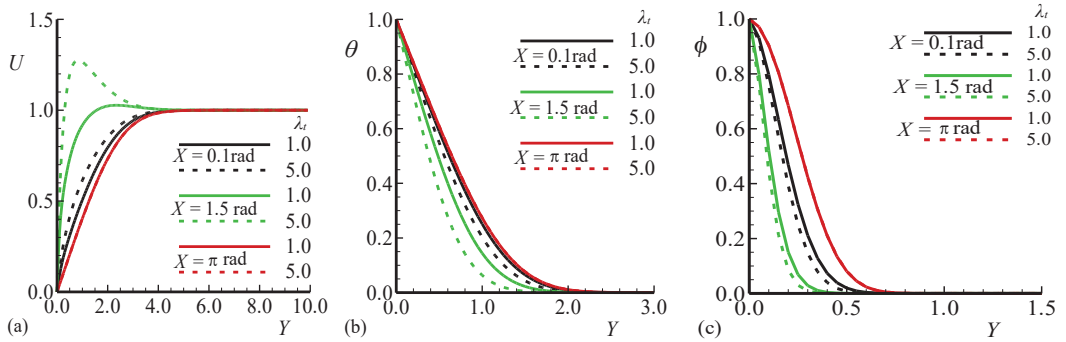

Figure 6. Graphical results of; (a) velocity profile (b) temperature profile, and (c) mass concentration against Y for different values of $\lambda_t = 1.0$, 5.0, when other prameters Pr = 7.0, $Nt = 10.0$, $\varepsilon = 1.0$, $\lambda_c = 1.0$, Sc = 10.0, and $k = 1.0$ are constant (*for color image see journal web site*)

why does this happen? It happens because the increase in mixed convection parameter leads to enhance buoyancy force that acts like a pressure gradient which ensures the above explained mechanism.

Figures 7(a)-7(c) represent the result plotted for variables U, θ and ϕ for various values of thermophoretic coefficient, k. For given values of parameter k, velocity profile is overall maximum at point $X = 1.5$ radian and is increased for increasing values of k. It is observed that temperature distribution and mass concentration is maximum at point $X = \pi$ radian and mass concentration is enhanced at this point for increasing values of k. Table 1 presents the result for skin friction, heat transfer, and mass flux for different values of viscosity parameter, ε, around different positions $X = 0.1, 0.2, 1.5, 2.5$ and π radians. We noticed from the analysis that skin friction is increased in middle range at points $X = 1.5, 2.5$ radians and enhanced for increasing value of $\varepsilon = 10.0$. Simlarly, the rate of heat transfer and mass concentrations are also maximum at the same previously mentioned points. Table 2 demonstrates the numerical results for the effects of various values of thermophoresis parameter $Nt = 1.0, 10.0$ around different positions of a sphere as described in tab. 1. From this table we observe that skin friction, heat transfer rate, and mass flux are maximum at positions $X = 1.5, 2.5$ radians, skin friction and rate of heat transfer are increased while mass flux is reduced with the increasing values of thermophoresis parameter.

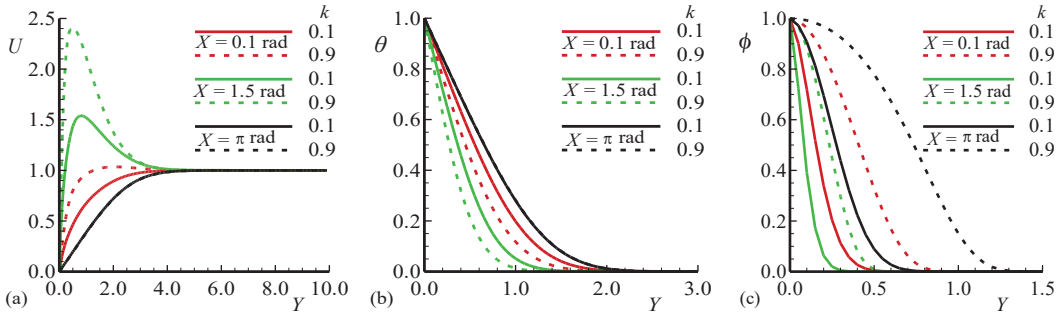

Figure 7. Graphical results of; (a) velocity profile (b) temperature profile, and (c) mass profile against Y for different values of thermophoretic coefficient k = 0.1, 10.0, when other parameters λ_t = 10.0, Pr = 7.0, Nt = 10.0, ε = 0.5, λ_c = 10.0, and Sc = 10.0 are constant (*for color image see journal web site*)

Table 1. Numerical results of skin friction, rate of heat transfer, and rate of mass transfer for various values of ε at different circumferential positions of a sphere, when other parameters λ_t = 10.0, λ_c = 10.0, Nt = 10.0, Sc = 10, k = 1.0, and Pr = 7.0 are constant

	$\left(\frac{\partial U}{\partial Y}\right)_{y=0}$		$\left(\frac{\partial \theta}{\partial Y}\right)_{y=0}$		$\left(\frac{\partial \phi}{\partial Y}\right)_{y=0}$	
X	$\varepsilon = 0.1$	$\varepsilon = 1.0$	$\varepsilon = 0.1$	$\varepsilon = 1.0$	$\varepsilon = 0.1$	$\varepsilon = 1.0$
0.1 rad.	1.87045	9.24316	1.12700	1.47863	0.00122	0.00909
1.5 rad.	9.48961	41.44794	1.85770	2.50490	0.00168	0.02102
2.0 rad.	9.48961	39.04457	1.81739	2.45036	0.00169	0.02045
2.5 rad.	6.53429	29.78918	1.64793	2.21957	0.00168	0.00037
π rad.	0.39002	0.36388	0.78004	0.79455	0.00053	0.00037

Table 2. Numerical results of skin friction, rate of heat transfer, and rate of mass transfer for various values of *Nt* at different cirmcumferential positions of a sphere, when other parameters $\lambda_t = 10.0$, $\lambda_c = 50.0$, $\varepsilon = 0.8$, Sc = 10.0, $k = 1.0$, and Pr = 7.0 are constant

	$\left(\frac{\partial U}{\partial Y}\right)_{y=0}$		$\left(\frac{\partial \theta}{\partial Y}\right)_{y=0}$		$\left(\frac{\partial \phi}{\partial Y}\right)_{y=0}$	
X	$Nt = 1.0$	$Nt = 10.0$	$Nt = 1.0$	$Nt = 10.0$	$Nt = 1.0$	$Nt = 10.0$
0.1 rad.	19.12283	19.62593	1.80628	1.96039	0.52203	0.01241
1.5 rad.	83.65838	88.07614	3.09419	3.40022	0.96959	0.03384
2.0 rad.	78.90581	82.96628	3.02651	3.32431	0.94573	0.02341
2.5 rad.	60.52075	63.26874	2.73965	3.00288	0.84550	0.01084
π rad.	0.18301	0.15695	0.77540	0.76421	0.08388	-0.00012

Conclusion

The present study is focused on the combined effects of variable viscosity and thermophoretic transportation on mixed convection flow. From the obtained results the following conclusions may be drawn.

It is noted that velocity profile increases owing to increase in viscosity variation parameter but the opposite behavior is seen in temperature distribution and mass concentration. It is revealed that the fluid velocity is increased significantly for higher values of thermophoresis parameter by keeping the other parameters constant. On the other hand, opposite behavior can be seen in temperature profile and mass concentration. It is noted that velocity of the fluid is increased at position $X = 1.5$ radian and gains its maximum value for Pr =0.71, while the temperature and mass concentration are reduced at the same position. For given values of parameter k, velocity profile is overall maximum at point $X = 1.5$ radian and is increased for increasing values of k. It is observed that temperature distribution and mass concentration is maximum at point $X = \pi$ radian and mass concentration is enhanced at this point for increasing values of k. We noticed from the analysis that skin friction is increased in middle range at points $X = 1.5, 2.5$ radians and enhanced for increasing value of $\varepsilon = 10.0$. Simlarly rate of heat transfer and mass concentrations are also maximum at the same previous mentioned points. We observe that skin friction, heat transfer and mass flux are maximum at positions $X = 1.5, 2.5$ radian, skin friction and rate of heat transfer are increased while mass flux is reduced with the increasing values of thermophoresis parameter.

Nomenclature

a – radius of a sphere, [m]
C – mass concentration in boundary layer, [kgm^{-3}]
D_m – mass diffusion coefficient, [m^{2}s^{-1}]
g – gravitational acceleration, [ms^{-2}]
$\bar{r}$ – dimensioned radial distance from the symmetric axis to the surface of a sphere, [m]
T – fluid temperature in boundary-layer, [K]
U – primitive variable for velocity component in X-direction
u – dimensionless velocity component in x-direction
V – primitive variable for velocity component in Y-direction
V_t – primitive variable for thermophoretic velocity
v_t – dimensionless thermophoretic velocity
v – dimensionless velocity component in y-direction
x, y – dimensionless axes along and normal to the surface of a sphere

Greek symbols

α – thermal diffusivity, [ms^{-1}]
β_c – volumetric coefficient concentration expansion, [K^{-1}]
β_t – volumetric coefficient thermal expansion, [K^{-1}]
γ – constant

ε – viscosity variation parameter
θ – dimensionless temperature
κ – thermal conductivity, [$Wm^{-1}K^{-1}$]
μ – dynamic viscosity, [Pas]
ν – kinematic viscosity, [m^2s^{-1}]
ϕ – dimensionless mass concentration

Subscripts

∞ – ambient conditions
w – wall conditions

References

[1] Potter, J. M., Riley, N., Free convection from a heated sphere at large Grashof number, *J. Fluid Mech*., *100* (1980), 4, pp. 769-783
[2] Epstein, M., *et al.,* Thermophoretic Deposition of Particles in Natural Convection Flow from a Vertical Plate, *Int. J. Heat Transfer,107* (1985), 2, pp. 272-276
[3] Attia, H. A., Unsteady Hydromagnetic Channel Flow of Dusty Fluid with Temperature Dependent Viscosity and Thermal Conductivity, *Heat Mass Transfer, 42* (2006), 9, pp. 779-787
[4] Chin, K. E., *et al.,* Effect of Variable Viscosity on Mixed Convection Boundary Layer in Porous Medium, *Int. Communications in Heat and Mass Transfer*, *34* (2007), 4, pp. 464-473
[5] El-Hakiem, M. A., Rashad, A. M., Effect of Radiation on Non-Darcy Free Convection from a Vertical Cylinder Embedded in a Fluid-Saturated Porous Medium with a Temperature-Dependent Viscosity, *J. Porous Media, 10* (2007), 2, pp. 209-218
[6] Enzo, Z., Mixed Convection with Variable Viscosity in a Vertical Annulus with Uniform Wall Temperatures, *Int. J. Heat and Mass Transfer*, *51* (2008), 1-2, pp. 30-40
[7] Perez, C. E., *et al.,* The Steady Navier-Stokes/Energy System with Temperature-Dependent Viscosity-Part-1: Analysis of the Continuous Problem, *Int. J. Numer. Meth. Fluids*, *56* (2008), 1, pp. 63-89
[8] Perez, C. E., *et al.,* The Steady Navier-Stokes/Energy System with Temperature-Dependent Viscosity-Part-2: The Discrete Problem and Numerical Experiments, *Int. J. Numer. Meth. Fluids*, *56* (2008), 1, 91-114
[9] Abe-El Aziz, M. S., Rania, F., Effects of Variable Viscosity and Suction/Injection on Thermal Boundary Layer of Non-Newtonian Power-Law Fluids Past a Power-Law Stretched Surface, *Thermal Science,14* (2010), 4, pp. 1111-1120
[10] Chamkha, A. J., *et al.,* Heat and Mass Transfer by Non-Darcy Free Convection from a Vertical Cylinder Embedded in Porous Media with Temperature Dependent Viscosity, *Int. J. Numerical Methods for Heat and Fluid Flow*, *21* (2011), 7, pp. 847-863
[11] Rashad, A. M., *et al.,* Effect of Chemical Reaction on Heat and Mass Transfer by Mixed Convection Flow about a Sphere in a Saturated Porous Media, *Int. J. Numerical Methods for Heat and Fluid Flow, 21* (2011), 4, pp. 418-433
[12] Chinyoka, T., Makinde. O. D., Unsteady Hydromagnetic Flow of a Reactive Variable Viscosity Third-Grade Fluid in a Channel with Convective Cooling, *Int. J. Numer. Meth. Fluids*, *69* (2012), 2, pp. 353-365
[13] Hayat, T., *et al.,* MHD Mixed Convection Peristaltic Flow with Variable Viscosity and Thermal Conductivity, *Sains Malaysiana*, *43* (2014), 10, pp. 1583-1590
[14] Crosby, A., Lister, J. R., Creeping Axisymmetric Plumes with Strongly Temperature-Dependent Viscosity, *J. Fluid Mech., 745* (2014), Apr., R2
[15] Dhiman, J. S., Sharma, N., Effects of Temperature Dependent Viscosity on Thermal Convection of Nanofluids: Steady Case, *J. Thermophysics and Heat Transfer*, *29* (2015), 1, pp. 90-101
[16] Lee , J., *et al.,* Turbulent Thermal Boundary Layers with Temperature Dependent Viscosity, *Int. J. Heat and Fluid Flow*, *14* (2014), Oct., pp. 43-52
[17] Umavathi, J. C., Ojjela. O., Effects of Variable Viscosity on Free Convection in a Vertical Rectangular Duct, *Int. J. Heat and Mass Transfer*, *84* (2015), 1, pp. 1-15
[18] Ashraf, M., *et al.,* Effects of Temperature Dependent Viscosity and Thermal Conductivity on Mixed Convection Flow along a Magnetized Verticsl Surface, *Int. J. Numerical Methods for Heat and Fluid Flow*, *26* (2015), 5, pp. 1580-1592
[19] Thoray, C., Michaut, C., Elastic-Plate Gravity Currents with a Temperature-Dependent Viscosity, *J. Fluid of Mechanics*, *805* (2016), 1, pp. 88-117
[20] Makinde, O. D., *et al.,* MHD Variable Reacting Flow over a Convectively Heated Plate in a Porous Medium with Thermophoresis and Radiative Heat Transfer, *Int. J. Heat and Mass Transfer*, *93* (2016), 1, pp. 595-604

[21] Malikarjuna, B., *et al.,* Transpiration and Thermophoresis Effects on Non-Darcy Convective Flow Past a Rotating Cone with Thermal Radiation, *Arabian Journal for Science and Engineering, 41* (2016), 11, pp. 4691-4700
[22] Ashraf, M., *et al.,* Periodic Momentum and Thermal Boundary Layer Mixed Convection Flow around the Surface of Heated Sphere in the Presence of Viscous Dissipation, *Cand. J. Phys*., *95* (2017), 10, pp. 976-986
[23] Ashraf, M., Fatima, A., Numericalsimulation of the Effect of Transient Shear Stress and the Rate of Heat Transfer around Different Positions of Sphere in the Presence of Viscous Dissipation, *J. Heat Transfer, (ASME),140* (2018), 6, pp. 701-7012
[24] Ashraf, M., *et al.,* Natural Convection Boundary Layer Flow of Nanofluids around Different Stations of Sphere and into Plume Above the Sphere, *Heat Transfer-Asian Research, 48* (2019), 3, pp. 1127-1148

Paper submitted: May 18, 2019
Paper revised: March 16, 2020
Paper accepted: March 19, 2020